Final Report on

Wireless Inter-Chip Signal Transmission by Electromagnetic Coupling of Open-Ring Resonators

Name of contractor	The University of Tokushima
Contract number	FA2386-10-1-4077
Report period	From April 19, 2010 to April 18, 2011

Authors Yasuo Ohno(Professor) and Mami Abe* (Graduate course student)
Institute of Technology and Science, The University of Tokushima
2-1 Minami-Josanjima, Tokushima 770-8506, Japan
E-mail: ohno@ee.tokushima-u.ac.jp
*present affiliation: Japan Aerospace Exploration Agency (JAXA.)

Abstract

For the measurement of wireless interconnection using open-ring resonator coupling at 60GHz band, photo mask patterns are designed. Also, electromagnetic simulations are carried out. The best transmission performance is estimated that the insertion loss of -1.85dB at 62.5 GHz with the 3dB bandwidth of 6.0GHz. The effect of wax layer for chip bonding is experimentally investigated.

1. Introduction

Due to the advance of device miniaturization, the device speed on chips has increased. In addition, as the application fields of electronic systems spread, functional integration has enhanced. Therefore, broad-band interconnections among different types of IC chips are required.

The conventional I/O interconnections, such as bonding wires, flip-chip bonding and pin connections, however, have drawbacks on the performance and reliability issues. Several new approaches have been proposed, including on-chip antennas, and capacitive or inductive coupling through circuits. All these structures needs signal re-generation or amplification, since the transmission loss is too large.

We proposed a resonator coupling with ring type λ/2 resonators [1]. Although the transmission distance is limited to the order of wavelength, the structure has high transmission efficiency and wide bandwidth. Since it is free from the rigid mechanical connection or precise alignment, it will solve the chip interconnection problems.

The purpose of this project is to confirm the availability of the open-ring resonator coupling by experiments. For the application on semiconductor chips, we will use sapphire as the common substrate. Sapphire is a good substrate for AlGaN/GaN HFET, but it is also used for silicon CMOS as SOS (silicon on sapphire). Also, the dielectric constant is similar to silicon, so the results are useful for the application to bulk silicon devices.

We designed the ring patterns [2] by layout editor "Ledit" together with their electromagnetic simulation results by HFSS.

2. Mask Design for 60GHz Band

2.1 Design Principle

We set the target frequency at 60GHz from three reasons. The open-ring diameter is $\lambda/2\pi$ where λ is the signal wavelength on the chips. On sapphire or silicon substrates, the diameter will be 240μm at 60 GHz. In regard to occupied area on the chip, the frequency will be the lower limit. The second reason is that the transmission distance is limited less than a fraction of the wavelength. The substrate thickness will not be thinned down to 100-200μm. Then, 60 GHz will be the upper limit. In addition, the band is quite open for new applications in every country. So, the frequency will cover wide area of applications. Therefore, the mask design starts with the frequency of 60GHz and the substrate of sapphire with the thickness of 200μm.

Report Documentation Page

Form Approved
OMB No. 0704-0188

1. REPORT DATE	2. REPORT TYPE	3. DATES COVERED
12 AUG 2011		

4. TITLE AND SUBTITLE	5a. CONTRACT NUMBER
Wireless Inter-Chip Signal Transmission by Electromagnetic Coupling of Open-Ring Resonators	5b. GRANT NUMBER
	5c. PROGRAM ELEMENT NUMBER
6. AUTHOR(S)	5d. PROJECT NUMBER
Yasuo Ohno	5e. TASK NUMBER
	5f. WORK UNIT NUMBER
7. PERFORMING ORGANIZATION NAME(S) AND ADDRESS(ES)	8. PERFORMING ORGANIZATION REPORT NUMBER
The University of Tokushima,2-1 Minami-Josanjima-cho,Tokushima-shi 770-8506,Japan,NA,NA	**N/A**
9. SPONSORING/MONITORING AGENCY NAME(S) AND ADDRESS(ES)	10. SPONSOR/MONITOR'S ACRONYM(S)
	11. SPONSOR/MONITOR'S REPORT NUMBER(S)

12. DISTRIBUTION/AVAILABILITY STATEMENT

Approved for public release; distribution unlimited.

13. SUPPLEMENTARY NOTES

14. ABSTRACT

For the measurement of wireless interconnection using open-ring resonator coupling at 60GHz band, photo mask patterns are designed. Also, electromagnetic simulations are carried out. The best transmission performance is estimated that the insertion loss of -1.85dB at 62.5 GHz with the 3dB bandwidth of 6.0GHz. The effect of wax layer for chip bonding is experimentally investigated.

15. SUBJECT TERMS

16. SECURITY CLASSIFICATION OF:			17. LIMITATION OF ABSTRACT	18. NUMBER OF PAGES	19a. NAME OF RESPONSIBLE PERSON
a. REPORT	b. ABSTRACT	c. THIS PAGE			
unclassified	**unclassified**	**unclassified**		**14**	

Standard Form 298 (Rev. 8-98)
Prescribed by ANSI Std Z39-18

2.2 Structure of the rings

Interconnection cross section view and top view are shown in Fig. 1 and 2. Three sapphire plates are stacked. Open-rings are placed on the top surfaces of the lower and the middle plates. On the surface of the upper plate, metal ground plane is formed. At the bottom of the lower plate, metal layer is also described, but actually, the metal stage of probing stations will be used instead. In this material, the wavelength of 60 GHz signal is 1.58 mm. Here, we assumed sapphire dielectric constant is $10\varepsilon_0$ for simplicity, but actually it is anisotropic with dielectric constant of $11.5\varepsilon_0$. This will only slightly affect the results.

Three patterns for the ring design are prepared as shown Fig. 3, long neck (A), short neck (b) and shielded ring (C). We expect that the radiation losses by parallel mode propagation will be different. Detailed design parameters are given in Fig. 2 and Table 1. Though the line impedances are determined by electrical design, there are flexibility in the line widths. Two designs are prepared, type-M and Y. The codes are given by the original designers' name, Mami and Yuka.

So, there are 6 different types of ring designs. For each type, several feeder line points specified as the insertion angles θ are prepared. The angles are varied from 20° to 110° because the optimum angle will vary dependent on the layer spacing and material properties.

2.3 Transmission characteristic simulation

Figures 4-9 show the transmission characteristics for the 6 structures, MA, MB, MC, YA, YB and YC. The sapphire interlayer thickness is 200μm, the metal conductivity is $4.1\text{x}10^7$S/m and "wave port" is assumed for the signal port. The results are summarized in Table 2. The best value is S21max of -1.85dB and bandwidth of 6.0GHz for the structure MA. The second is YC. For YC, the best angle is 58° which data is shown in Fig. 10. From these results, the short neck maybe not good and sufficient space maybe needed around the rings.

To evaluate the loss mechanism, perfect conductor (PEC) is assumed for the metals as shown in Figs. 11-16. The results are also included in Table 2. The degradation by the metal resistance is about 0.5dB for M structures and 1dB for Y structures.

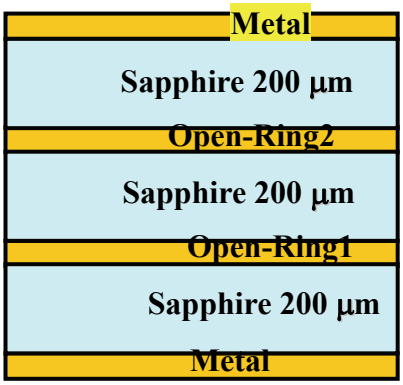

Fig. 1 Interconnection structure cross section view. Sapphire thickness is assumed 150μm or 200μm.

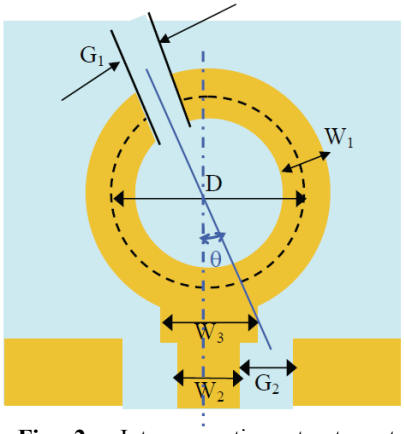

Fig. 2 Interconnection structure top view.

(a) Type-A (b) Type-B (c) Type-C

Fig. 3 Ring part structures. (a) Type-A, long neck, (b) Type-B, short neck and (c) Type-C, shielded.

Table 1 Design values for the two feeder line types.
Two types, M and Y are designed where the line widths are different.

Type	ring			feeder line		
				neck part (MSL)	to port part (CPL)	
	D (μm)	W_1 (μm)	G_1 (μm)	W_3 (μm)	W_2 (μm)	G_2 (μm)
M(Mami)	240	95	30	95	70	120
Y(Yuka)	240	45	20	45	45	63

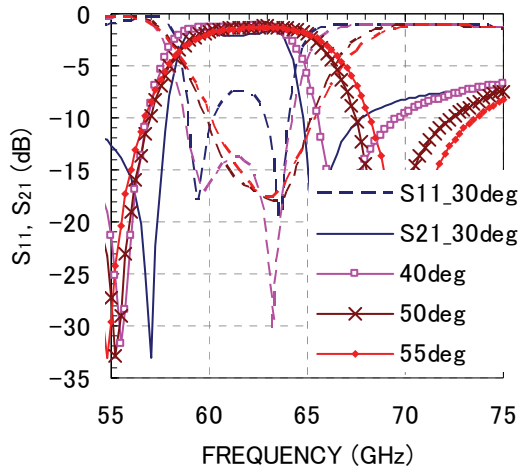

(a)

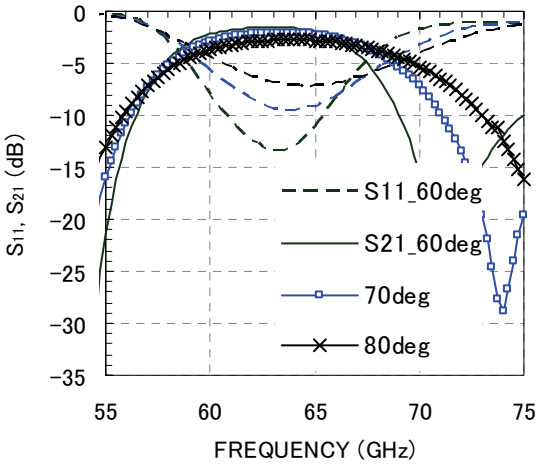

(b)

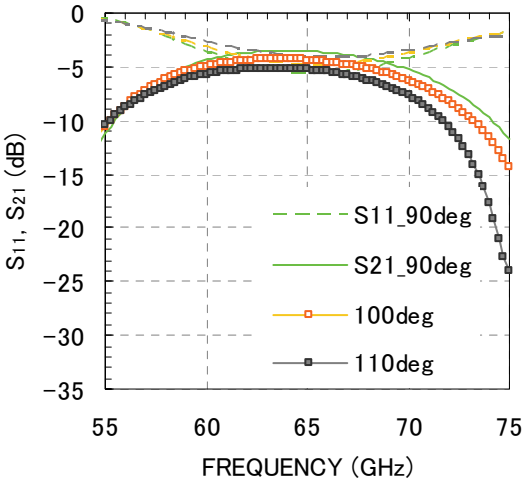

(c)

Fig. 4 Feeder insertion angle dependencies for MA structure. (a) 30°, 40°, 50°, 55°, (b) 60°, 70°, 80° and (c) 90°, 100°, 110°.

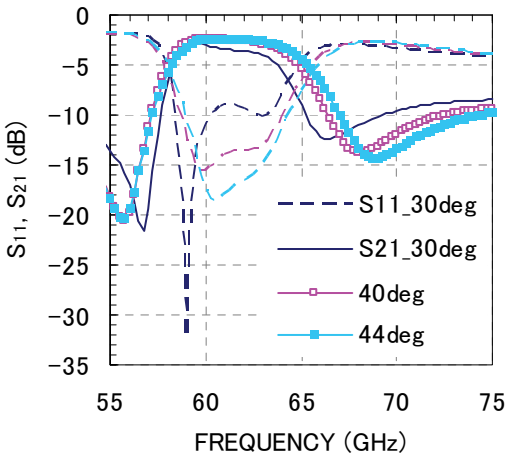

(a)

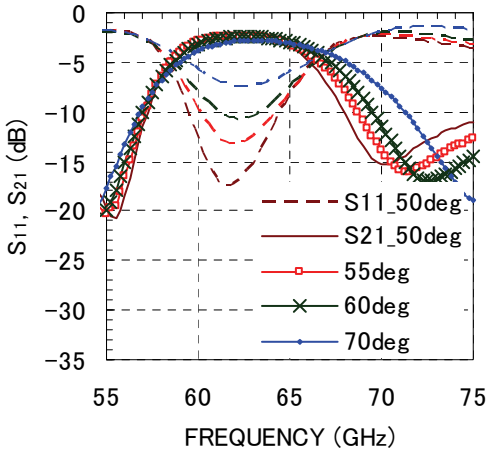

(b)

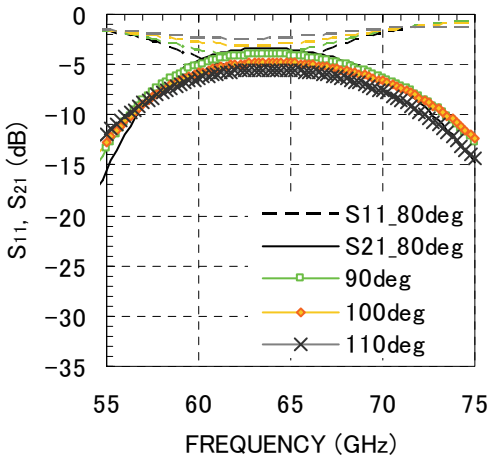

(c)

Fig. 5 Feeder insertion angle dependencies for MB structure. (a) 30°, 40°, 44°, (b) 50°, 55°, 60°, 70° and (c) 80°, 90°, 100°, 110°.

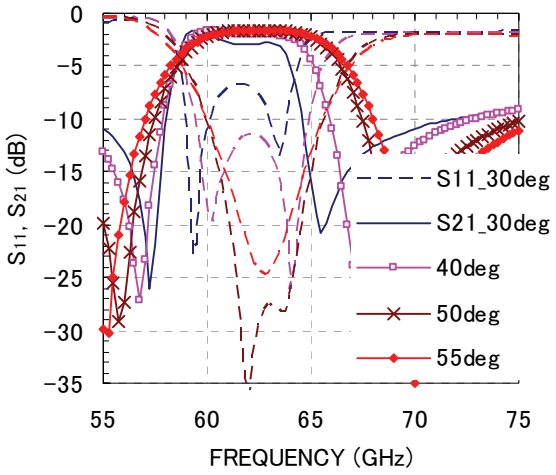

(a)

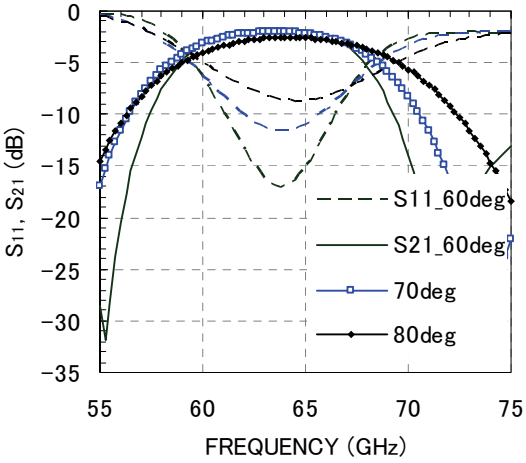

(b)

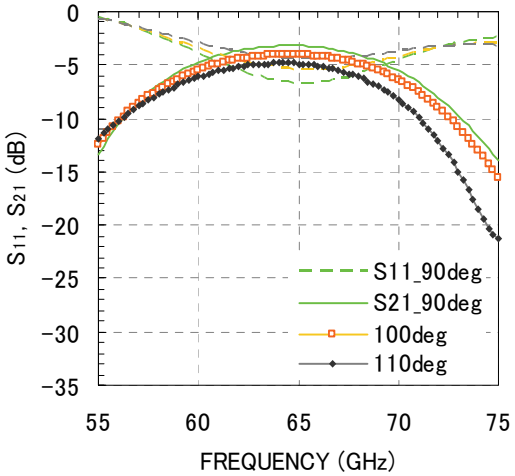

(c)

Fig. 6 Feeder insertion angle dependencies for MC structure. (a) 30°, 40°, 50°, 55°, (b) 60°, 70°, 80° and (c) 90°, 100°, 110°.

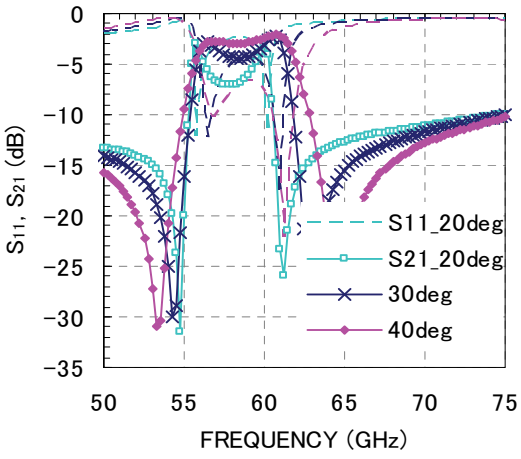

(a)

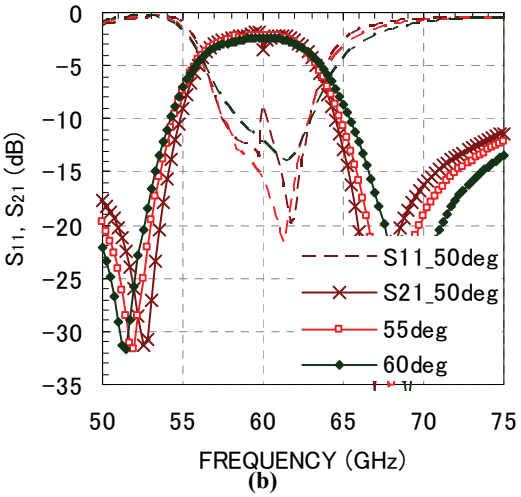

(b)

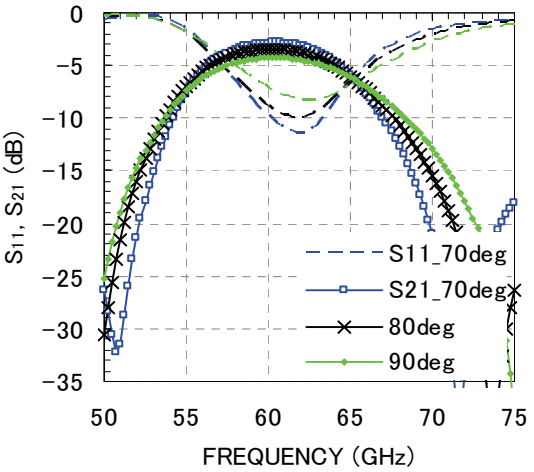

(c)

Fig. 7 Feeder insertion angle dependencies for YA structure. (a) 20°, 30°, 40°, (b) 50°, 55°, 60° and (c) 70°, 80°, 90°.

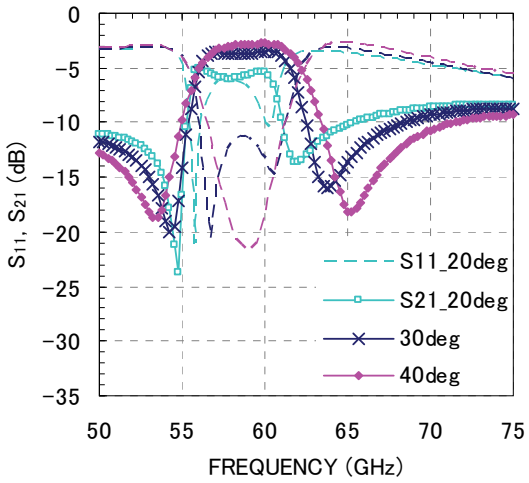

(a)

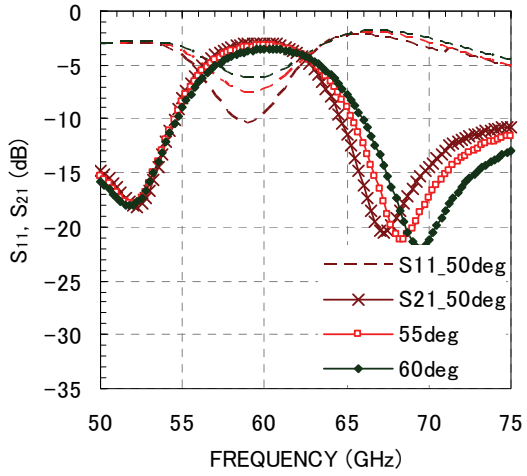

(b)

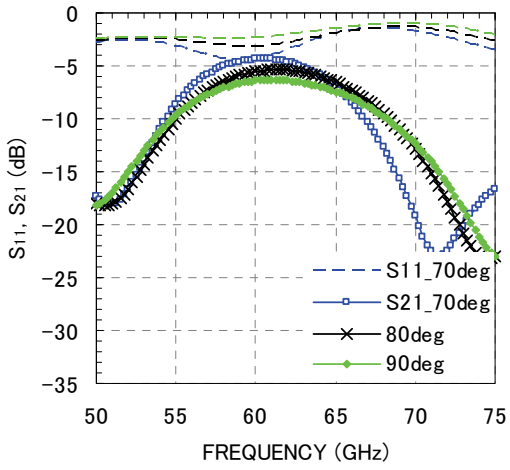

(c)

Fig. 8 Feeder insertion angle dependencies for YB structure. (a) 20°, 30°, 40°, (b) 50°, 55°, 60° and (c) 70°, 80°, 90°.

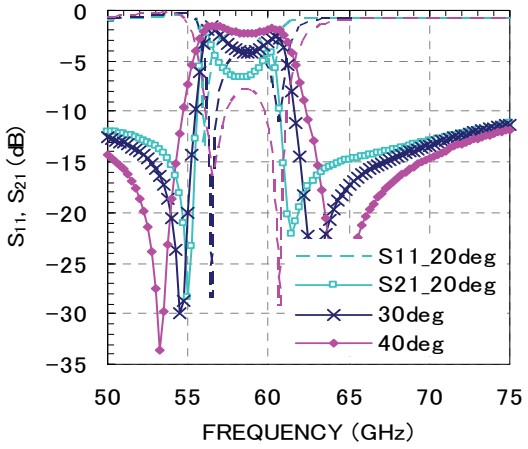

(a)

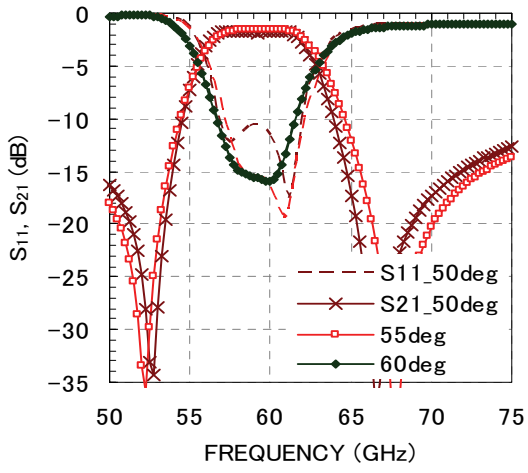

(b)

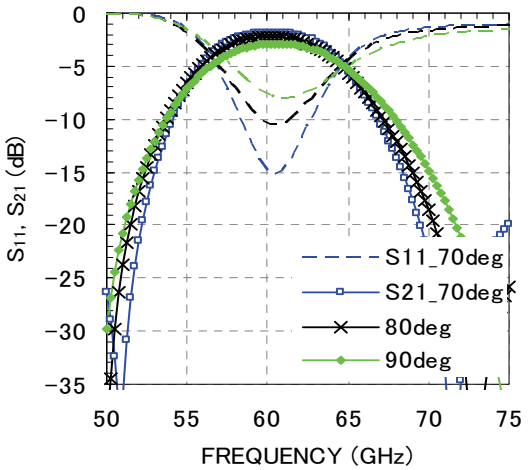

(c)

Fig. 9 Feeder insertion angle dependencies for YC structure. (a) 20°, 30°, 40°, (b) 50°, 55°, 60° and (c) 70°, 80° 90°.

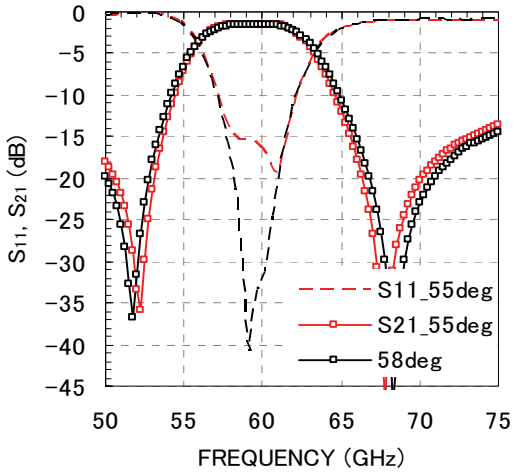

Fig. 10 Comparison of feeder insertion angle of 55° and 58° for YC.

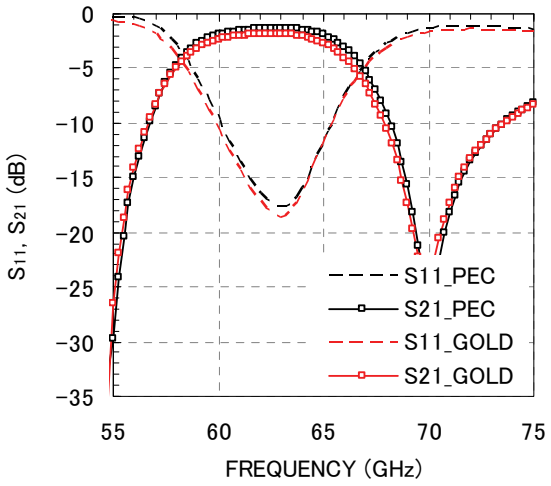

Fig. 11 Effect of metal conductivity. Simulations are carried out for MA structure at θ=55°.

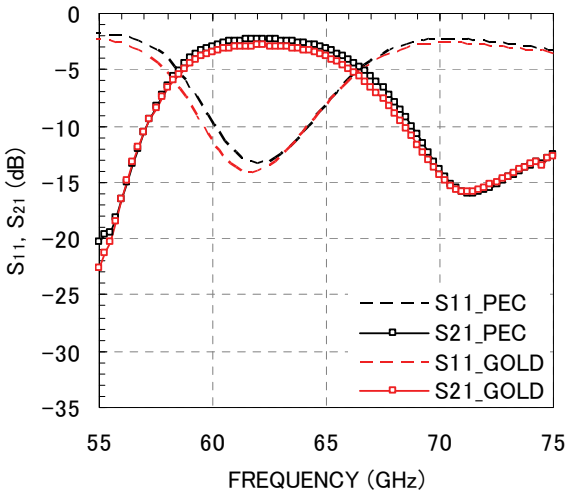

Fig. 12 Effect of metal conductivity. Simulations are carried out for MB structure at θ=55°.

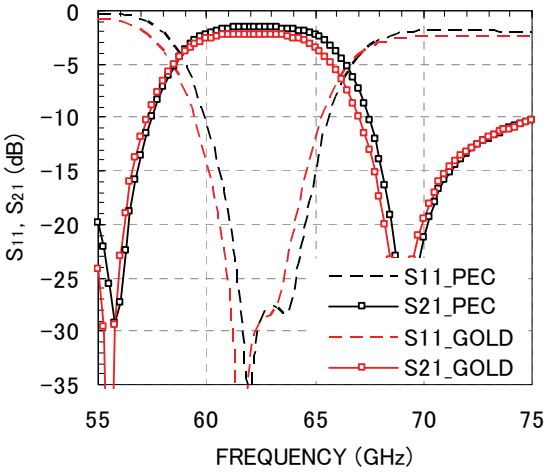

Fig. 13 Effect of metal conductivity. Simulations are carried out for MC structure at θ=50°.

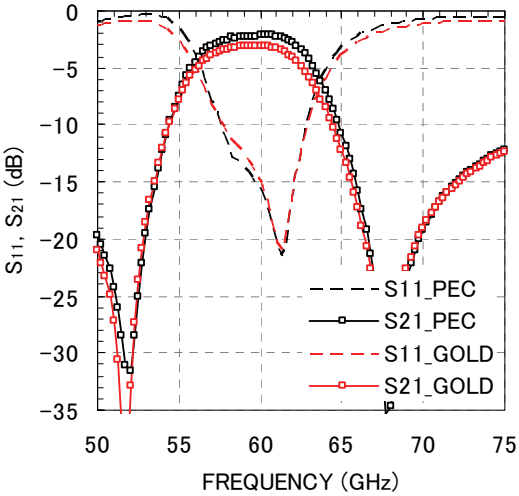

Fig. 14 Effect of metal conductivity. Simulations are carried out for YA structure at θ=55°.

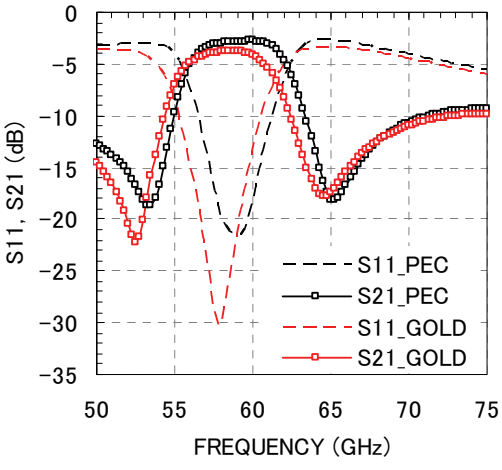

Fig. 15 Effect of metal conductivity. Simulations are carried out for YB structure at θ=40°.

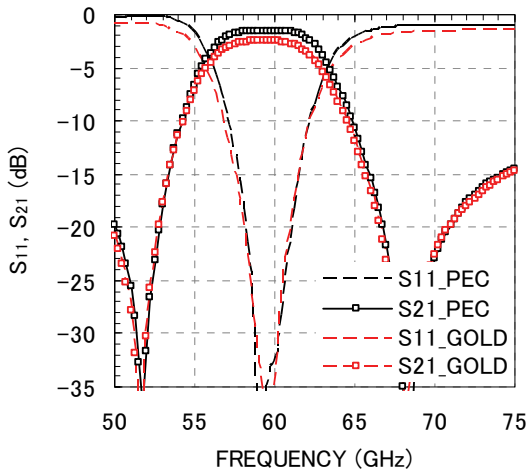

Fig. 16 Effect of metal conductivity. Simulations are carried out for YC structure at θ=58°.

Table 2　Summary of simulation result for the designed structures.
Data show the minimum loss conditions. Metal loss is obtained from the S21max values　for PEC and Gold.

Structure	metal	angle (degree)	bandwidth (GHz)	S21max (dB)	frequency (GHz)	metal loss (dB)
MA	PEC	55	6.75	−1.35	62.75	0.50
	Gold	55	6.00	−1.85	62.50	
MB	PEC	55	4.75	−2.36	62.25	0.52
	Gold	55	2.00	−2.88	62.00	
MC	PEC	50	6.00	−1.60	62.00	0.59
	Gold	50	4.75	−2.19	62.00	
YA	PEC	55	4.75	−2.17	60.25	0.89
	Gold	55	0.00	−3.06	59.75	
YB	PEC	40	2.75	−2.77	59.75	1.00
	Gold	40	0.00	−3.77	58.75	
YC	PEC	58	6.00	−1.50	60.00	0.97
	Gold	58	4.00	−2.47	59.50	

2.4 Effect of port condition for simulation results

Above simulations are carried out assuming “wave port.” In “wave port,” there is no reflection at the port. In actual measurement, however, the probes touches only at a finite area and some reflections may occur.. To simulate this situation, “lumped port” can be used. Figure 17 shows the difference of the two port conditions. The result using “lumped port” gave always 1-2dB worse results.

Simulations are carried out for a simple 50Ω transmission lines. The metal is assumed as PEC.

Loss estimated by $1-|S_{11}|^2-|S_{21}|^2$ at 60GHz is 1.2% for "wave port," while it is 28.1% for lumped port. We do not know which is appropriate for actual situations, but we should keep it in mind as the origin of simulation error.

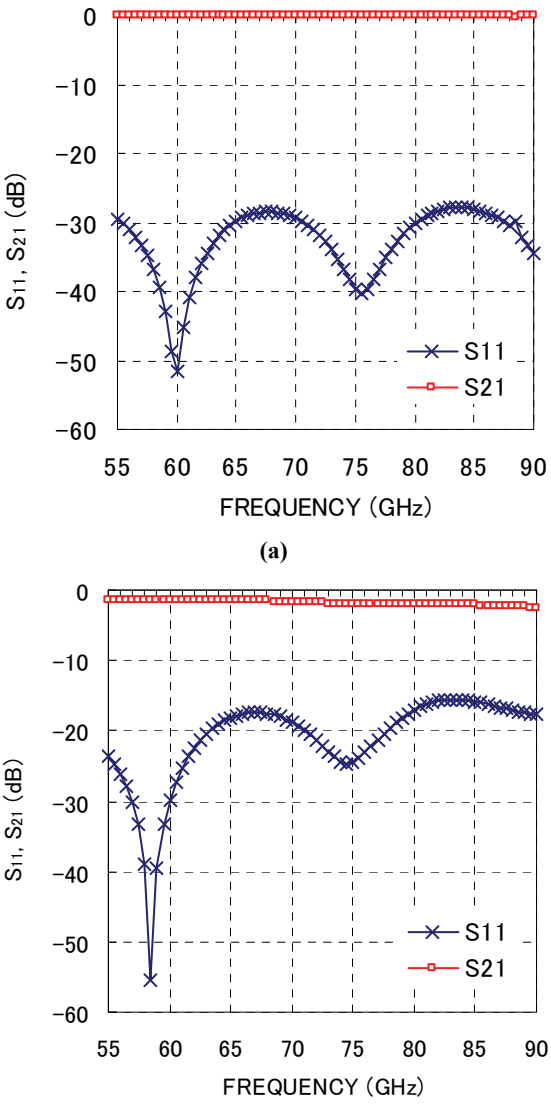

Fig. 17 Comparison of port condition for simulation. (a) Wave port, (b) Lumped port.

2.5 Chip layout

Figure 18 shows the schematic cross section of measurement structure. Figure 19 shows the mask patters of the chips. The chip size is 32mm x 34.4mm which is designed for a single chip on one 2 inchϕ wafer. One resonator pattern occupies 3.0 x 4.3mm square. There are 100μm wide space lines in the ground planes between the devices to eliminate the effects of unintended reflections.

After metal patterning, the wafer will be cut into pieces, where 20 devices are installed on one sub-chip. Then, the sub-chips are stacked and fixed by wax and goes to measurement.

On the mask, simple transmission line patterns with the characteristic impedance form 30 to 80Ω are prepared to check the material parameters and the accuracy of the fabricated patterns.

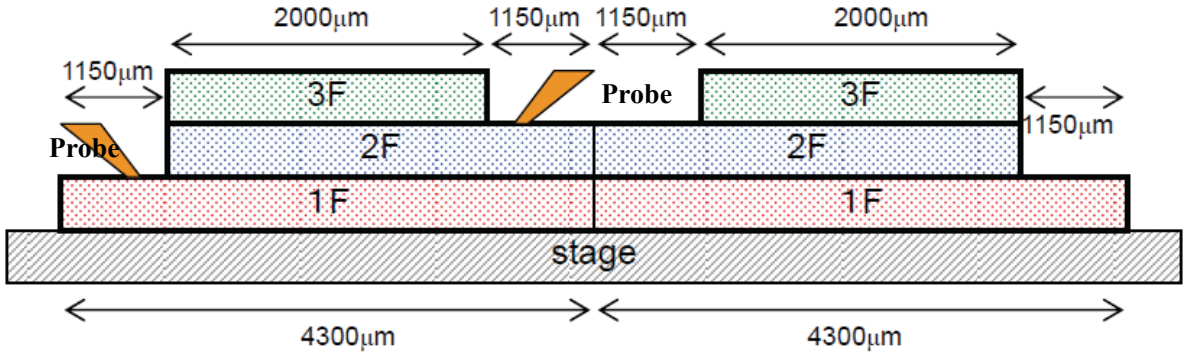

Fig. 18 Schematic cross section of experiment structure. Chips made by three mask layers, 1F, 2F, 3F are stacked. Prove needles are put on the pads on 1F and 2F chips. Chip sizes are shown.

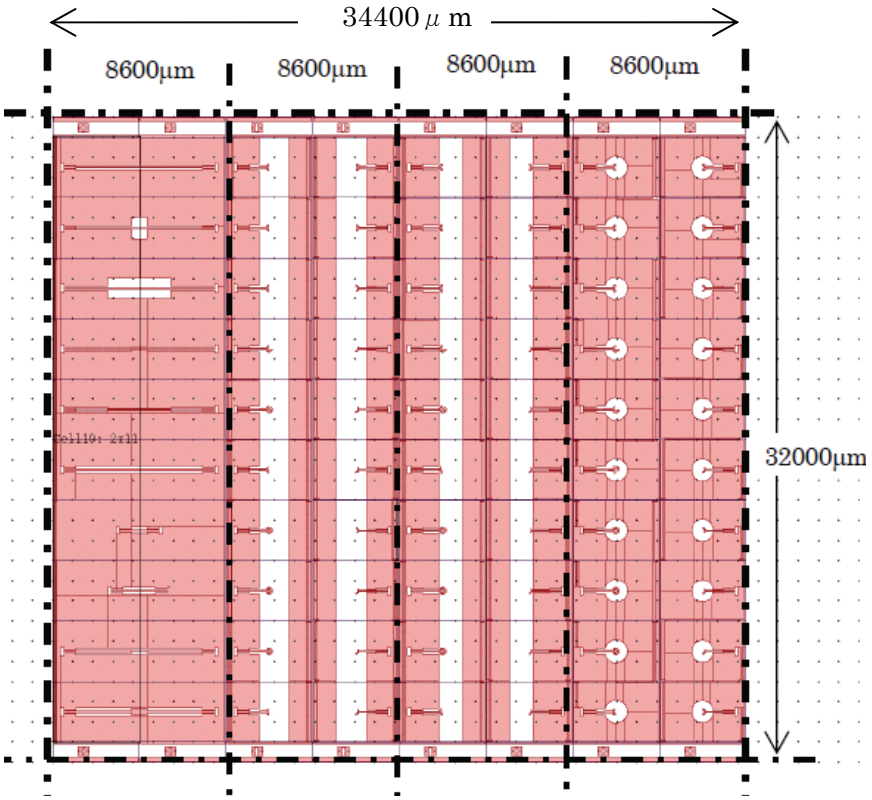

Fig. 19 (a) Mask pattern of layer 1F, lower ring layer. Lnes indicate the cutting position for scribing.

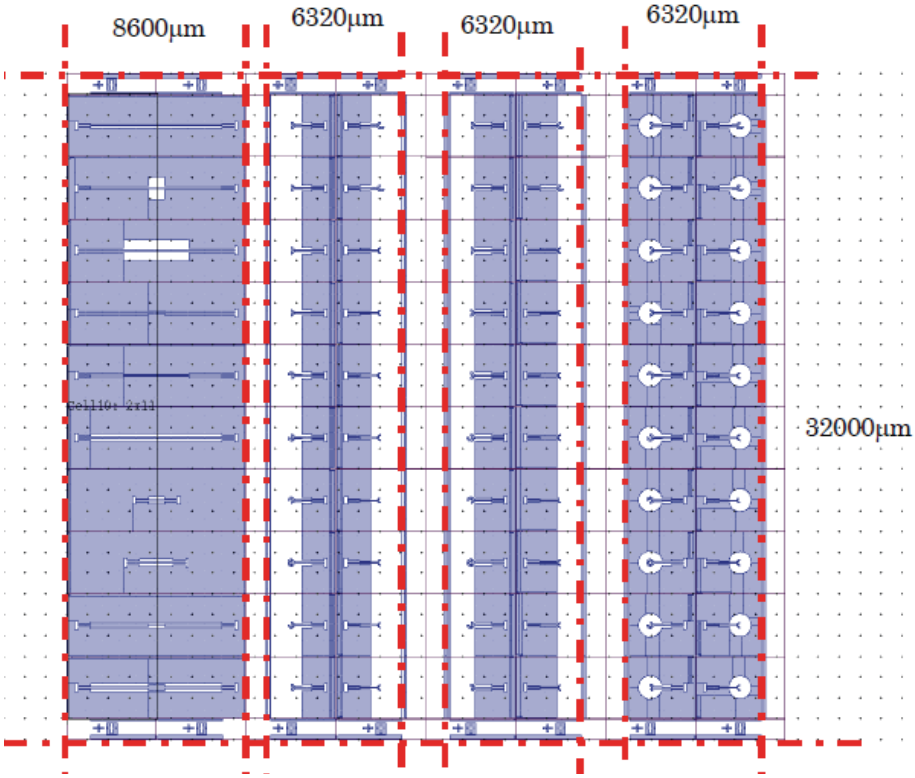

Fig. 19 (b) Mask pattern of layer 2F, upper ring layer. Red lines indicate the cutting position for scribing.

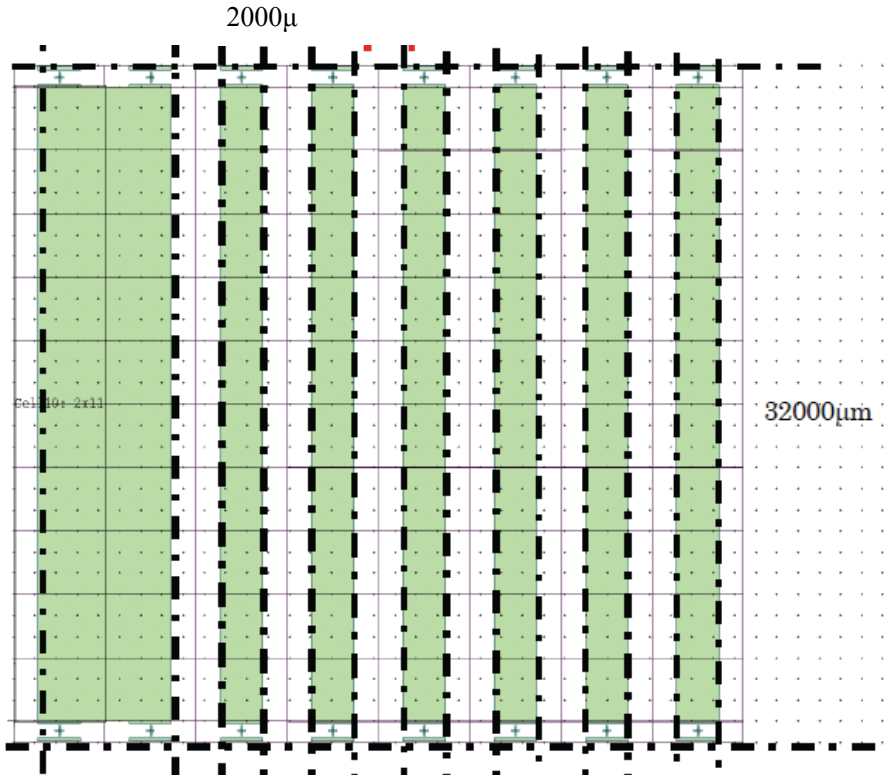

Fig. 19 (c) Mask pattern of layer 3F, top shielding layer. Lnes indicate the cutting position for scribing.

3. Problems in chip bonding

In 15GHz experiment, the resonant frequencies are normally about 20% higher than the simulated value. We suspected the wax layer between sapphire substrate may be the origin. Figure 20 is our chip mounting equipment. In the chip mounting, we coat wax diluted by acetone on the lower chip surface by spinner. On the aligner stage, we put the upper chip on the accurate position of the lower chip, and then, heat the chips by lamp or hair dryer. Dr G. Jessen suggested that insufficient melting of the wax will contain air bubbles between the substrates. Therefore, we compared the performance before and after the additional heat treatment. Heat treatment is done at 110°C for 5 min where the chips are bonded by metal paper-clips. Then, milky white color disappeared and become transparent. However, the measured stacked wafer thickness is still 50μm, thicker than the twice of the single wafer thickness.

Figure 22 shows the measurement results. After the wax melting, center frequency shifted to 2 to 3 GHz downwards. Due to the increased coupling coefficient, the bandwidth is also increased.

From this result, the actual chip may contain certain wax layers. So, the designed values for 200μm thick sapphire substrate is not fit to the actual substrate, but fit to thinner substrate.

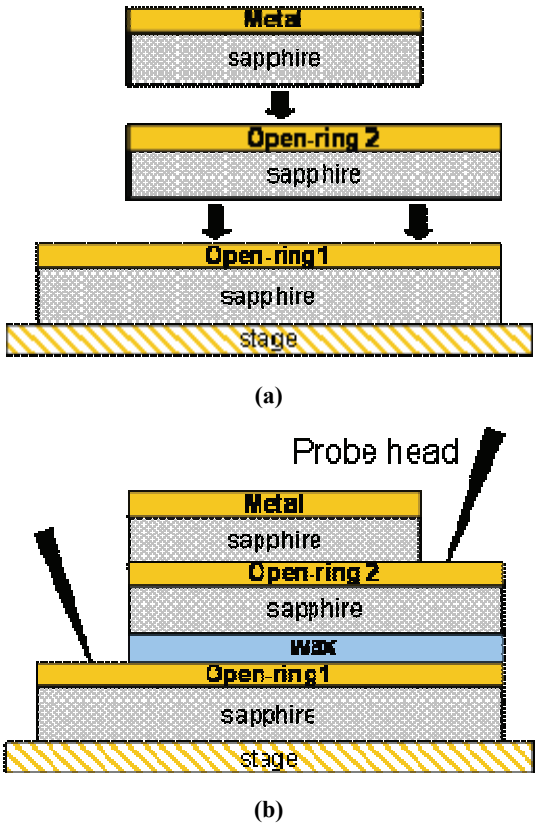

Fig. 21 Cross section views of chip mounting. (a) Before mounting, (b) after mounting. Wax layers for the chip bonding form a layer with lower dielectric constant.

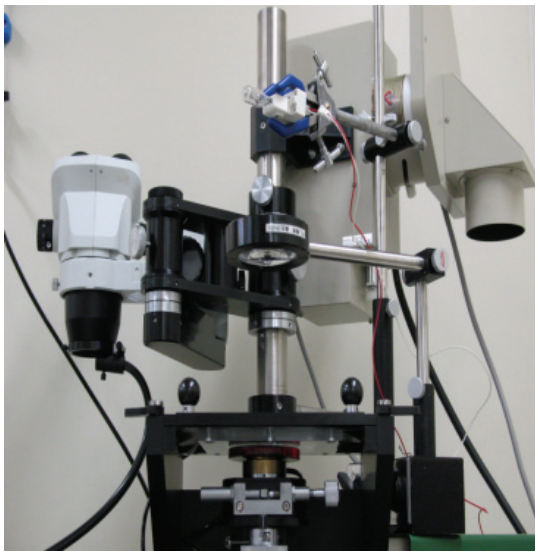

Fig. 20 Chip mounting alignment machine converted from mask aligner.

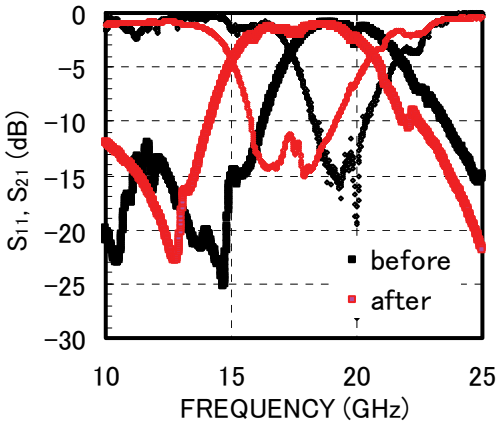

Fig. 22 Effect of wax condition. By melting the wax, transmission band shift about 1.5 GHz downwards and the band width increased.

4. Conclusion

Open-ring wireless interconnection is designed for the small signal measurement at 60 GHz range. Patterns are divided into 3 neck part structures and 2 feeder line designs. For the 6 patterns MA, MB, MC, YA, YB and YC, different feeder insertion angles are prepared. For each patterns, HFSS simulations are carried out.

From the simulation results, the best performance is obtained as the loss of -1.85 dB and the bandwidth of 6.00 GHz. From the simulation, the loss by metal resistance is -0.5dB for M patterns and -1dB for Y pattern. The simulations also include ambiguity by the port conditions as around 0.5dB.

In the actual measurement, the wax for the chip adhesion will affect the performance.

Acknowledgements

We would like to thank Ms. Yuka Okuyama and Ms. Mami Abe for the design and simulation works of the interconnections.

We would also like to thank Dr. James Gillespie, Electronics Engineer, Aerospace Components Division, Dr. Tony K. Quach, Mixed signal Technology Manager, and Dr. Dennis E. Walker, Jr., Chief Scientist, Aerospace Group, WYLE, and Dr. Gregg Jessen, AOARD, for their support for this project and valuable discussion.

References

[1] Y. Ohno and I. Awai, “Wireless Interconnection by Electromagnetic Coupling of Open-Ring Resonators and Its Application to System,” *2009 International Conference on Solid State Devices and Materials(SSDM 2009)*, D-2-1

[2] Yasuo Ohno, Mami Abe, " Design Reports on MASK ECOR 03," Inhouse report, Dec 31, 2011

Publications

1. J. -P. Ao, et. al.,"S-parameter Analysis of GaN Schottky Diodes for Microwave Power Rectification," *32nd IEEE Compound Semiconductor IC Symposium*(*CSICS 2010*), Montrey, USA, J-4 (2010)

2. M. Abe, T. Amou, K. Kuramoto, J.-P. Ao, Y. Ohno, "Effects of Substrate Conductivity on Open-Ring Resonator Wireless Interconnection," 2010 Asia-Pacific Radio Science Conference, (AP-RASC'10), D1-6, Toyama, Japan(2010)

3. Mami Abe, Yuka Okuyama, Jin-ping Ao, "Misalignment effects in inter-chip wireless connection with open-ring resonators," 2010 Asia-Pacific Microwave Conference Proceedings, (APMC 2010), 908 - 911, Yokohama, Japan(2010)

4. Yasuo Ohno, "Application of GaN Devices to Wireless Power Transmission," 2010 Asia-Pacific Microwave Conference Proceedings, (APMC 2010), WS2A-1, Yokohama, Japan(2010)

5. K. Harauchi, et. al., "Power Transmission through Insulating Plate Using Open-Ring Resonator Coupling and GaN Schottky Diode, " *IMWS-IWPT 2011,* May 12-13, 2011 – Uji (Kyoto), Japan, IWPT2-2 (2011)

6. Yasuo Ohno and Jing-Pin Ao, "Microwave Power Transmission Using Open-ring Resonators Coupling and GaN SBD," 2011 Asia_Pacific Workshop on Fundametals and Applications of advanced semiconductor devices (AWAD 2011), June 29- July 1 , 2011, Daejeon, Korea(2011)